ELSEVIER

Biophysical Chemistry 77 (1999) 1–8

Biophysical Chemistry

Effects of solvent perturbation on gelation driven by spinodal demixing

D. Bulone[a,c], A. Emanuele[b,c], P.L. San Biagio[a,b,c,*]

[a] *CNR-Istituto per le Applicazioni Interdisciplinari della Fisica, Via U. La Malfa, 153-I90146 Palermo, Italy*
[b] *Department of Physical and Astronomical Sciences, University of Palermo, Palermo, Italy*
[c] *INFM at the Department of Physical and Astronomical Sciences, Via Archirafi, 36-I90123 Palermo, Italy*

Received 12 July 1998; accepted 12 September 1998

Abstract

We study effects of solvent perturbation on kinetic competition between spinodal demixing and gelation in agarose solutions at a concentration of 5 g/l. Two different cosolutes (*tert*-butyl alcohol and trimethyl amine *N*-oxide) known for altering in opposite way solvent-mediated interactions are chosen. By rheometry, static and dynamic light scattering experiments, we show that the cosolute presence shifts the boundary of the instability region of solution leaving unaffected temperature and polymer concentration values required for percolation. Results suggest that an appropriate choice of quenching temperature and solvent allows controlling the gelation time and the gel structural properties.

Keywords: Gelation; Spinodal demixing; Agarose; Phase transition; Polymer physics

1. Introduction

In the last few years, gels gained a considerable relevance in the field of material science from both theoretical and practical points of view [1–8]. The name *gel* is ascribed to a variety of diverse systems characterized by the presence of a liquid-bearing percolative structure exhibiting a solid like behavior in specific conditions (temperature, pH, concentration, solvent, etc.). Structural properties of gel are of high interest for technological purposes: for example, in food technology a particular structure is required in relation to the taste of the product; clear and soft gels are appreciated for cosmetic and pharmaceutical purposes; spreadable gels are required in paints and pastes industries and gels with a controllable pore dimension are useful in biotechnology for biomolecule sieving and separation. This has prompted a lot of efforts for the understanding of the relationship between structural properties of gels and the physical or chemical processes involved in gelation [9–15].

Structural properties of covalently bonded (chemical) gels are usually controlled by choosing

* Corresponding author. e-mail: sbiagio@iaif.pa.cnr.it.

0301-4622/99/$ - see front matter
PII: S0301-4622(99)00004-6

the appropriate polymer, cross-link agent and solvent fraction [16]. Chemical gels are typically homogeneous and their formation can be well described through percolation theory [3,7,17]. In physical gels polymeric aggregation is reversible due to dependence of the interactions involved (hydrogen bonding, van der Waals or hydrophobic interactions) on temperature, pH, solvent, ionic strength, etc. [18]. The fact that cross-linking is reversible makes gel structural properties highly dependent upon the samples thermal history and the experimental conditions in which the gel is formed.

Formation of physical gels from polymeric solutions can occur even at concentrations well below the threshold for random cross-links percolation [13,19–23]. In these conditions, solute–solute correlations necessary for non-random cross-linking are provided by the thermodynamic phase transition of demixing. Spontaneous concentration fluctuations onset by quenching the polymer solution inside its instability region generate lower and higher than average concentration regions. Depending on the total polymer concentration, domains of high concentration, where cross-linking is favored, may remain mutually disconnected [24–26] or may assemble in a percolative structure [13,19–23]. In the first case, gelation occurs only on a mesoscopic scale and gel aggregates are observed to diffuse freely in a macroscopic liquid [24,25]. In the second case, the macroscopic gel shows inhomogeneous microstructure due to a mesoscopic pattern imposed by the demixing process [13,27–30]. As shown by experiments and computer simulation [28,31–33], the relative time scale of demixing and gelation processes determines gel structural properties.

In a recent work [15] we studied the role and interplay of different processes (spinodal demixing, conformational transition, cross-linking) involved in the gelation of a representative biopolysaccharide, the agarose. The complete, quantitative phase diagram for this system is reported and discussed in San Biagio et al. [13]. Agarose is an essentially uncharged polysaccharide obtained from marine red seaweed often used in studies of physical gelation processes. It has a molecular weight in the order of 100 000 and the structure of an altering copolymer of 3-linked-D-galactopyranose and 4-linked 3,5-anhydro-α-L-galactopyranose residues [34,35]. We found that kinetic competition and multiple interactions between the three processes involved in gelation are responsible for a variety of gel structures that can be obtained quenching the same sample at different temperature values [15].

In the present work, techniques of solvent perturbation are used to modulate demixing and gelation processes in aqueous agarose solutions and also to figure out how this can alter the final structure of the gel. Two cosolutes [*tert*-butyl alcohol (TBOH) and trimethyl amine-*N*-oxide (TMAO)] known for altering in opposite way, solute–solute interactions [36,37] were chosen. Demixing and gelation kinetics were followed applying concurrently different techniques on the same samples. Data show that the kinetic competition between demixing and gelation can be altered by choosing the solvent and/or the temperature appropriately. This controls, in turn, the final structure of gel.

2. Materials and methods

2.1. Sample preparation

Agarose was Ultrapure Seakem HGT(P) from FMC BioProducts, Rockland, ME, lot no. 62933, with a nominal sulfate content less then 0.15%. Water was Millipore Super Q filtered with 0.22-μm filters. Agarose water solution at a concentration of 5 g/l was put into a sealed tube and kept in boiling water for 20 min with occasional gentle mixing (autoclaving at higher temperature was avoided to prevent breaking of agarose chains, as previously reported [19]). For samples with 1% (molar fraction) TBOH (from Merk), the appropriate volumes of alcohol were first filtered at room temperature, heated to 80°C and added to the agarose solution prepared as above and stored at 80°C. Samples with 1% (molar fraction) TMAO (from Sigma Chemical Co.) were prepared in a different way: the agarose powder was weighed in a tube with approximately half of the amount of water required for a final agarose concentration of 5 g/l. The remaining water was used to dis-

solve the appropriate quantity of TMAO and was stored at 80°C. Agarose solution was boiled as above and finally mixed with TMAO solution. After preparation, the samples (if necessary) were stored at 80°C for not more than 2 h before starting the experiments. Samples were then quenched to the measurement temperature and experiments were begun after a 10-min period to allow for thermal equilibration. When appropriate, monodisperse polystyrene latex spheres (PLS) of a 60-nm nominal radius (Polyscience, Warrington, PA) were added at 80°C and at a final concentration of approximately 30 g/ml. Under these conditions, the light scattered by PLS was at least 10 times more than that from agarose. Sticking of agarose molecules to PLS can be ruled out as shown by previous work [19].

2.2. Dynamic and static light scattering experiments

Light scattered intensity and time autocorrelation function were measured using a Brookhaven Instruments 2030-AT 128-channel digital correlator, and an ILT 550 Argon laser tuned at 514.5 nm. Sample prepared as described above was put into a thermostatted cell compartment of a Brookhaven Instruments BI200-SM goniometer system. Temperature was controlled to within ± 0.1°C using a thermostatted recirculating bath. On following gelation kinetics, data were collected on different regions of the specimen by using a motor-driven cell holder. Structure function $S(q)$ was obtained by recording light scattered intensity at a different scattering vector $q = 4\ \pi\ n\ \lambda_0^{-1} \sin(\theta/2)$, where n is the refractive index of the solution, λ_0 is the wavelength of the incident light and θ is the scattering angle. Measurements were recorded over the angular range of 15–160° resulting in a q range from 0.032 to 0.004 nm^{-1}. Time autocorrelation functions were analyzed as previously reported [24–26] for diffusion coefficient, amplitude of correlation function and mean scattered intensity.

2.3. Viscosity and viscoelasticity measurements

Viscosity measurements were performed using a computer-interfaced Couette-type viscometer (Contraves Low-Shear 30). Available (constant) shear-rates, S, are in the range 1.6×10^{-2}–1.2×10^{2} sec^{-1}, the sample gap was 0.5 mm. Viscoelasticity measurements were made using a Rheometrics RFSII using a standard Couette tool, in this case the sample gap was 1 mm. Both instruments have a temperature-controlled recirculating bath to keep the sample temperature within ± 0.1°C.

3. Results and discussion

Agarose solutions at 5 g/l in pure water and in the presence of the two different cosolutes were quenched to various temperatures. The scattered light at 90° was monitored as a function of time. As known from previous work, when the spinodal decomposition of the solution becomes observable (e.g. by the appearance of a characteristic low-angle pattern in scattered light), the character of the light intensity fluctuations scattered at 90° changes abruptly [19]. The delay time for the appearance of this change can be taken as a measure of the characteristic time of spinodal decomposition. Fig. 1 shows the delay time dependence upon quench temperature for the three solvents used. In each case, the observed divergence allows one to derive the corresponding spinodal temperatures. The smooth curves drawn in the figure are best fits to the expression:

$$t = \left(\frac{To - T}{To} \right)^{-\gamma} \tag{1}$$

where To is the spinodal temperature and γ is a critical exponent. Values of To are: 47.3°C (1% TBOH), 49.8°C (H_2O) and 53.7°C (1% TMAO). The same value for A (≈ 0.68) and γ (1.3) are found. This implies that curves relative to 1% of TBOH and 1% of TMAO are displaced with respect to that of pure water by a constant -2.5°C and $+3.9$°C, respectively. Therefore the opposite effects of the two cosolutes on the early stage of spinodal decomposition can be traced to changes of the Flory-Huggins χ parameter expressing the difference between free energies of interactions between like and unlike species [38]. The sign of spinodal temperature shift is that expected on the basis that the two cosolutes used in the present

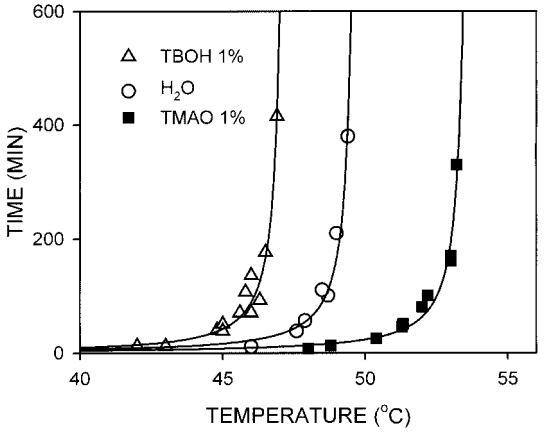

Fig. 1. Dependence upon temperature and solvent of the delay time for observing the change in light intensity fluctuations (see text). The continuous lines are the best fits to Eq. (1) yielding the same values for both A and γ. Temperatures at divergence points correspond to spinodal temperatures of 47.3°C, 49.8°C and 53.7°C.

work are known to alter in opposite way to solute–solvent interactions, decreasing or increasing the thermodynamic cost of keeping solutes exposed to the solvent [36,37].

Cosolutes effects on the structural properties of the solution in the course of spinodal demixing can be investigated by shear viscosity measurements [39–41]. It has been reported that on quenching a polymer solution inside its instability regions, a large transient surge of shear viscosity is observed after the same delay time required for the stabilization of the characteristic low-angle pattern in scattered light. At this time the sample is a macroscopic liquid and gelation starts much later. The large size of the viscosity surge and its inverse power-law dependence on the shear rate S pointed out the existence of a relaxation time τ such that $S\tau > 1$ [42,43]. It has been shown that this time is related to the characteristic length L_m of the pattern of high and low concentration domains developing in the course of spinodal demixing. Relevance of the associated characteristic time τ_m was confirmed by observing that viscosity peak values for different polymer concentration and quenching temperatures lie on a master curve when plotted vs. $(S\tau_m)^{-1}$ [39–41]. This evidence that the viscous dissipation is due to distortion and disruption by shear of some interdomains links or correlations. The same type of experiment was performed in the present work on agarose solution in different solvents. For a given solution and quenching temperature, a constant shear rate was applied immediately after quenching and the viscosity η was recorded; the experiment was repeated at different shear rate values. In Fig. 2, values of the viscosity surge relative to the initial viscosity of the solution $(\Delta\eta/\eta)$ are plotted vs. $(S\tau_m)^{-1}$. Values of τ for each solvent condition were obtained from Cahn's plots as previously described [39]. The observed master curve behavior states that the structural properties of the decomposed solutions are dictated by the characteristic length/time imposed by spinodal demixing. It has to be noted that scaled value of $\Delta\eta/\eta$ measured at the same quenching depth, which corresponds to the same τ_m, does not show any significant difference within experimental errors. That is, the three solutions quenched at the same depth inside their instability regions show in the course of spinodal demixing the same mechanical response to shear perturbation.

The above results indicate that the shift of the phase boundaries is the only effect of solvent perturbation in the first stages of the process leading to gelation. Cosolute effects on subsequent stages were therefore studied by performing comparison experiments on samples in different solvents quenched at the same depth inside their instability regions. This condition is equivalent to select temperatures corresponding to the same waiting time. This time was chosen to be 100 min to allow kinetic studies. Corresponding temperatures were $T = 45.8$°C for the water + TBOH solvent, $T = 48.3$°C for the pure water solvent and $T = 52.2$°C for the water + TMAO solvent.

In a first set of experiments the mobility of latex spheres (PLS) added to the samples as a function of time were measured. In Fig. 3, we report the amplitude of the autocorrelation function of light scattered by PLS measured in the first 800 min after the quenching. Only the sample containing TBOH shows a decrease of the amplitude starting approximately 500 min after

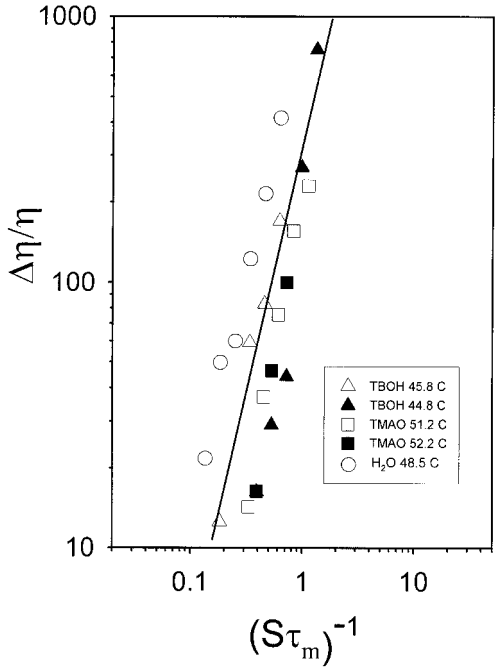

Fig. 2. Log–log plot of the viscosity peak values, $\Delta\eta/\eta$, vs. a scaled shear $(S\tau_m)^{-1}$; τ_m is the relaxation time associated with the interdomain structure, $\tau = (K_B\ T)^{-1}\ 6\pi\eta\ L_m^3$ [42,43], and L_m is independently measured by light scattering in each experimental condition reported in the figure legend.

quenching. That is, an increasing amount of PLS does not move freely in the solution well after spinodal demixing has matured. This amplitude decrease, due to hindrance of the PLS motion, could be a sign of an incipient cross-linking. As the sample is still a macroscopic liquid, cross-linking can occur only on a mesoscopic scale. Indeed, formation of mesoscopic gel aggregates could be responsible for an increased entanglement of solution.

Structural properties in the course of self-assembly were also studied by measurements of fractal dimension. Development of a self-similar structure of cross-linked molecules has been observed in agarose solution at higher concentration [14,15]. It occurs simultaneously with the formation of the larger scale structure of high concentration domains resulting from spinodal demixing. Polymer cross-linking initially occurs on the smaller scale corresponding to the size of the gel building blocks. These, in the case of agarose, are bundles of double helices with dimension (Lp) of the order of 0.1 μm [19,27,44]. The large scale structure is characterized by $L_m = 2\ \pi/q_m$ corresponding to the maximum of the distribution of interdomains distances. In the agarose case typical values of L_m are of the order of several micrometers. For q values such that $Lp < 2\pi q^{-1} < L_m$, the structure function $S(q)$ is featureless and follows the power-law dependence $S(q) \approx q^{-d_f}$. Here d_f is the mass fractal dimension defined by the relation $M \sim r^{df}$, where M is the mass of objects with radius r [45,46]. Kinetic studies on 20 g/l agarose solution in pure water showed that fractal dimension of the smaller scale structure grows from a very low value corresponding to unconnected scattering objects up to a final value of 1.2/1.4 at the gel point [14,15]. Typical times for gelation in such conditions range from minutes up to a few hours.

In our case, much longer gelation times are expected. For a point of reference at 5 g/l in pure water rapid macroscopic gelation occurs when the sample is quenched at 34°C [27]. Several weeks are instead, necessary at 49°C [27]. The three samples were quenched at the same depth and scattered light was recorded as a function of angle and time. In the case of pure water and 1% TMAO the fractal dimension is not observable up to 48 h after quenching. In the case of 1% TBOH

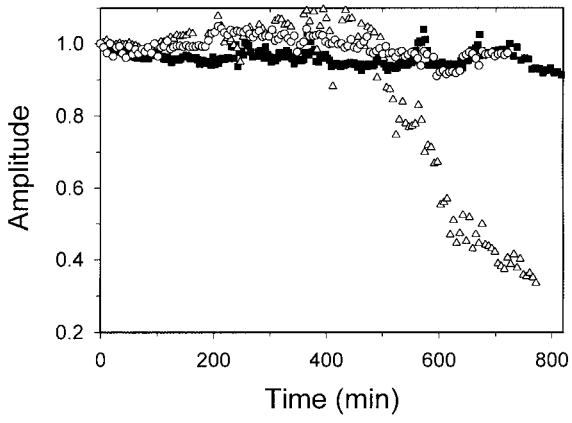

Fig. 3. Amplitude of the correlation function vs. time for the three samples quenched at the same depth inside their instability regions. Quenching temperatures are 45.8°C for 1% TBOH, 48.3°C for H_2O and 52.2°C for 1% TMAO. Symbols are the same as in Fig. 1.

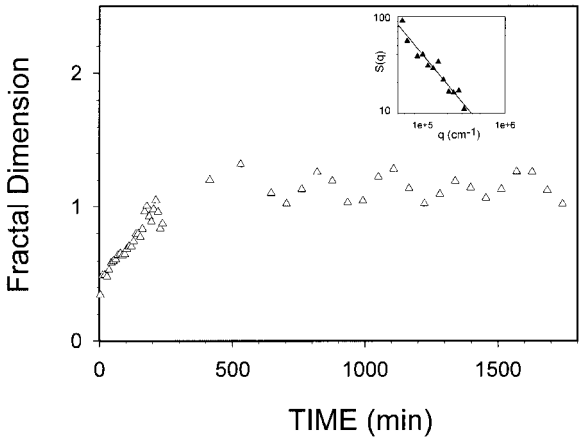

Fig. 4. Fractal dimension vs. time in 1% TBOH quenched at 45.8°C. The inset shows a typical log–log plot of structure function; the straight line is the best fit and fractal dimension is obtained from its slope.

shown in Fig. 4 the fractal dimension is observed to reach the value of 1.2 after approximately 8 h. Interestingly this is the same time at which the amplitude of light scattering correlation function (shown in Fig. 3) starts to decrease.

Mechanical properties of the demixed solutions at later stages of spinodal demixing were compared by measuring the viscoelastic properties of solutions at approximately 1500 min after quenching. Viscoelastic spectra reported in Fig. 5 are typical of entangled polymer solutions with the characteristic plateau in a narrow frequency region and ideal chain behavior at low and high frequencies. In the frame of reptation model the G′ value at plateau G(0) is proportional to temperature and depends on parameters describing the entanglement degree [47,48]. No three samples studied here appear to be a gel in the mechanical sense; thus, the mechanical properties of these samples are dominated by entanglement inside the high concentration domains developed by spinodal demixing. Finding a higher G(0) value for the sample (1% TBOH) quenched at lower temperature implies that this solution is the more rigid, as expected. A small quantity of cross-linking could be responsible for this.

In a further set of experiments, gelation kinetics are followed for longer times by a drop ball method. After approximately 4 days, sample containing TBOH appears as a macroscopic (although very weak) gel. After the same time, the other two samples are still a macroscopic liquid.

Altogether the above results show that: (1) the spinodal demixing of solutions in these experimental conditions is, in all cases, the first event in the process leading to gelation; (2) the presence of cosolutes shifts the instability line leaving unchanged the scaling behavior and the scale invariance of the shear dependence; and (3) gelation of samples quenched at the same depth inside their instability regions occurs on a different time scale. It should be noted that the same quenching depth corresponds to equal demixing kinetics and characteristic length. Although the pattern of low and high concentration regions is the same, preceeding of cross-linking (favored in polymer-rich regions) and percolation take different times. This suggests that the shift of the spinodal line by cosolutes is not paralleled by an analogous effect on the gelation line. In fact, if the number and

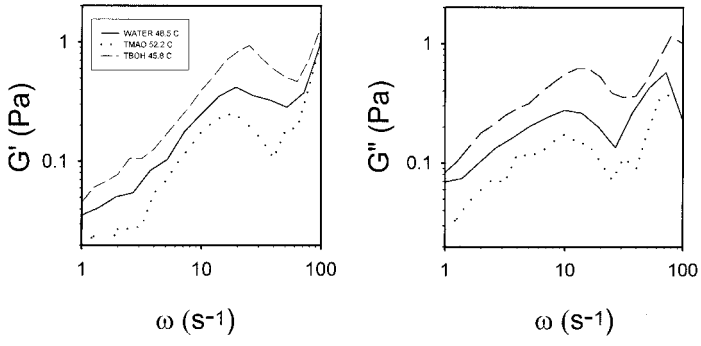

Fig. 5. Log–log plots of G′ and G″ vs. ω (sec^{-1}) in different solvents at the same quenching depth.

energy of bonds are not affected by cosolutes, the dependence of bonding/non-bonding equilibrium upon temperature and polymer concentration is not changed. This implies that a smaller concentration value for starting cross-links percolation is required at lower temperature. As the kinetics of spinodal demixing is the same for the three samples quenched at the same depth, gelation will be faster for the sample quenched at lower temperature.

As a check of the above interpretation, we performed a further set of experiments on the three samples quenched at the same temperature, that is at the same distance (in the T,c plane) from the gelation line. In this case, the concentration value for starting percolation should be the same, but demixing kinetics would be faster for a deeper quenching. Therefore the three samples are expected to become gels with a different gelation time and different structural properties. In Fig. 6 we report kinetic growing of the fractal dimension observed in the three solutions all quenched at 45.8°C. Macroscopic gelation is observed in all cases. It occurs in the 1% TMAO case after about the same time (200 min) at which the fractal dimension reaches a stationary value. In pure water, gelation occurs after approximately 1400 min. The 1% TBOH case has been already discussed with reference to Fig. 4. Data show that the fractal dimension is greater for a deeper quenching depth. This agrees with a more compact structure dictated by the smaller characteristic length.

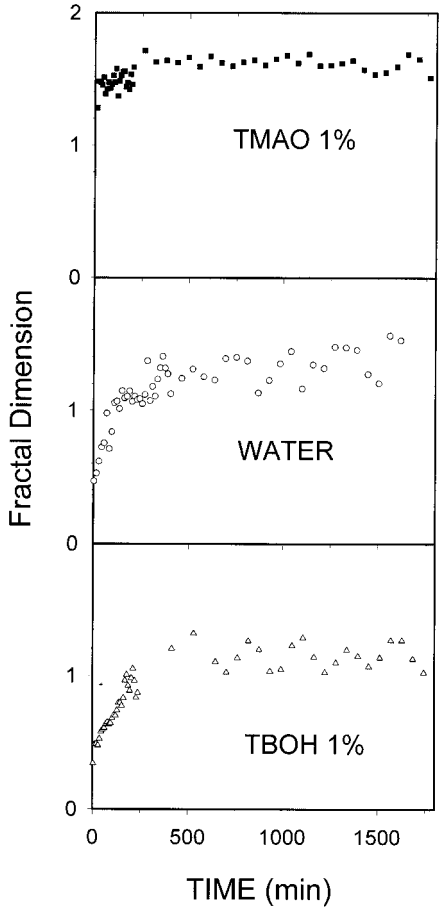

Fig. 6. Fractal dimension (derived as reported in Fig. 4) vs. time in different solvents quenched at the same temperature (T = 45.8°C).

4. Conclusions

We studied kinetic competition between spinodal demixing of the solution (thermodynamic transition) and cross-linking and aggregation (topological transition) in the presence of small cosolutes. The chosen experimental conditions are such that the spinodal demixing in each case is the first dominant step in promoting non-random cross-linking and percolation.

Results reported show that modulation of solute–solvent interactions shifts the boundary of the instability region accordingly with that expected by single thermodynamic considerations; instead, temperature dependence of concentration threshold for percolation does not seem affected by cosolute presence. Therefore with an appropriate choice of solvent and quenching temperature it is possible to modulate the kinetic competition between demixing and gelation. This, in turn, allows the control of gelation time and gel structural properties: a more homogeneous gel structure can be obtained at the same quenching temperature by decreasing the goodness of a solvent or, a gel with the same structural properties can be obtained in less time by choosing a better solvent and quenching at lower temperature.

Acknowledgements

We thank Professors M.U. Palma and M.B. Palma-Vittorelli and Drs V. Martorana and M. Manno for helpful discussions and suggestions. The expert technical assistance of Dr D. Giacomazza, Mrs R. Megna, G. Lapis and M. Lapis is also acknowledged.

The present work was done at IAIF-CNR and University Laboratories. Partial support from the Italian 'Ministero per l'Universitá e per la Ricerca Scientifica e Tecnologica' and from the Sicilian 'Comitato Regionale Ricerche Nucleari e Struttura della Materia' is also gratefully acknowledged.

References

[1] W. Burchard, S.B. Ross-Murphy, Physical Networks Elsevier, London, 1988.
[2] A.H. Clark, in: S.E. Harding, S. Hills, J.R. Mitchell (Eds.), Biopolymer Mixtures, Nottingham University Press, Nottingham, 1996, p. 37.
[3] P.G. de Gennes, Scaling Concepts in Polymer Physics, Cornell University Press, Ithaca, NY, 1979.
[4] M. Kolb, M.A.D. Axelos, in: H.E. Stanley, N. Ostrowsky (Eds.), Correlation and Connectivity, NATO ASI Series E, Applied Sciences, vol. 188, Kluver Acad. Pub., Amsterdam, 1990, p. 255.
[5] J.E. Martin, D. Adolf, Ann. Rev. Phys. Chem. 42 (1991) 311.
[6] J.R. Mitchell, D.A. Ledward, Functional Properties of Food Macromolecules, Elsevier, London, 1985.
[7] D. Stauffer, A. Aharony, Introduction to Percolation Theory, Taylor and Francis, Bristol, 1991.
[8] M. Djabourov, Polymer Int. 25 (1991) 135.
[9] C.J. Brinker, G.W. Scherer, Sol-Gel Science, Academic Press, San Diego, CA, USA, 1990.
[10] J. Prost, F. Rondelez, Nature 350 (1991) 11.
[11] H.B. Bohidar, S. Maity, Eur. Polym. J. 34 (1998) 1361.
[12] T.A. Vilgis, H.H. Winter, Colloid Polym. Sci. 266 (1988) 494.
[13] P.L. San Biagio, D. Bulone, A. Emanuele, M.B. Palma-Vittorelli, M.U. Palma, Food Hydrocolloids 10 (1996) 91.
[14] M. Manno, M.U. Palma, Phys. Rev. Lett. 79 (1997) 4286.
[15] M. Manno, A. Emanuele, V. Martorana, D. Bulone, P.L. San Biagio, M.B. Palma-Vittorelli, M.U. Palma, Phys. Rev. E, in press.
[16] M. Doi, Introduction to Polymer Physics, Clarendon Press, Oxford, 1996, Chap. 3.
[17] P.J. Flory, Principles of Polymer Chemistry, Cornell University Press, New York, 1953.
[18] P.S. Russo (Ed.), Reversible Polymeric Gels and Related Systems, ACS Symp. Ser. 350, Washington D.C., 1987.
[19] P.L. San Biagio, F. Madonia, J. Newman, M.U. Palma, Biopolymers 25 (1986) 2255.
[20] A. Emanuele, L. Di Stefano, D. Giacomazza, M. Trapanese, M.B. Palma-Vittorelli, M.U. Palma, Biopolymers 31 (1991) 859.
[21] P.L. San Biagio, M.U. Palma, Biophys. J. 60 (1991) 508.
[22] F. Sciortino, K.U. Prasad, D.W. Urry, M.U. Palma, Biopolymers 33 (1993) 743.
[23] P.L. San Biagio, D. Bulone, A. Emanuele, M.U. Palma, Biophys. J. 70 (1996) 494.
[24] D. Bulone, P.L. San Biagio, Chem. Phys. Lett. 179 (1991) 339.
[25] D. Bulone, P.L. San Biagio, Biophys. J. 68 (1995) 1569.
[26] D. Bulone, J. Newman, P.L. San Biagio, Biophys. J. 72 (1997) 388.
[27] M. Leone, F. Sciortino, M. Migliore, S.L. Fornili, M.B. Palma-Vittorelli, Biopolymers 26 (1987) 743.
[28] R. Bansil, J. Lal, D. Carvalho, Polymer 33 (1992) 2961.
[29] F. Sciortino, R. Bansil, H.E. Stanley, P. Alstrøn, Phys. Rev. E 47 (1993) 4615.
[30] A.H. Clark, in: S.E. Harding, S. Hills, J.R. Mitchell (Eds.), Biopolymer Mixtures, Nottingham University Press, Nottingham, England, 1996, p. 37.
[31] S.C. Glotzer, M.F. Gyure, F. Sciortino, A. Coniglio, H.E. Stanley, Phys. Rev. E 49 (1994) 247.
[32] S. Hayward, D.W. Heermann, K. Binder, J. Stat. Phys. 49 (1987) 1053.
[33] Y. Liu, R.B. Pandey, J. Chem. Phys. 105 (1996) 825.
[34] C. Araki, K. Arai, Bull. Chem. Soc. Jpn. 40 (1967) 1452.
[35] L.S. Lerman, H.L. Frish, Biopolymers 21 (1982) 995.
[36] D. Bulone, P.L. San Biagio, M.B. Palma-Vittorelli, M.U. Palma, J. Mol. Liq. 58 (1993) 129.
[37] M.U. Palma, P.L. San Biagio, D. Bulone, M.B. Palma-Vittorelli, in: M.C. Bellissant-Funel, J.C. Dore (Eds.), Hydrogen Bond Networks, Kluwer Acad. Pub., Amsterdam, The Netherlands, 1994, p. 457.
[38] M. Kurata, Thermodynamics of Polymer Solutions, Harwood Acad. Pub., Chur, Switzerland, 1982.
[39] A. Emanuele, M.B. Palma-Vittorelli, Phys. Rev. Lett. 69 (1982) 81.
[40] A. Emanuele, M.B. Palma-Vittorelli, Int. J. Thermophys. 16 (1995) 363.
[41] A. Emanuele, M.B. Palma-Vittorelli, in: A.I. Nakatany, M.D. Dadmun (Eds.), Flow-induced Structure in Polymers, ACS Symp. Ser., Washington DC, 1995, p. 61.
[42] A. Onuki, Physica (Amsterdam) 140a (1986) 204.
[43] A. Onuki, Phys. Rev. A 35 (1987) 5149.
[44] S. Arnott, A. Fulmer, W.E. Scott, J. Mol. Biol. 90 (1974) 269.
[45] S.K. Sinha, Physica (Amsterdam) 38d (1989) 310.
[46] P.-z. Wong, Q.-z. Kao, Phys. Rev. B 45 (1992) 7627.
[47] M. Doi, S.F. Edwards, The Theory of Polymer Dynamics, Oxford University Press, Oxford, England, 1986.
[48] P.G. deGennes, J. Chem. Phys. 55 (1971) 572.